



## Aerosol Characteristics in the Three Poles of the Earth Observed by CALIPSO

5 Yikun Yang<sup>1,2</sup>, Chuanfeng Zhao<sup>1,2</sup>, Quan Wang<sup>3</sup>, Zhiyuan Cong<sup>4</sup>, Xingchun Yang<sup>1,2</sup>,  
Hao Fan<sup>1,2</sup>

<sup>1</sup>College of Global Change and Earth System Science, State Key Laboratory of Earth Surface Processes and Resource Ecology, Beijing Normal University, Beijing 100875, China

<sup>2</sup>Joint Center for Global Change Studies, Beijing Normal University, Beijing 100875, China

<sup>3</sup>Department of Atmospheric Physics, Nanjing University, Nanjing 210046, China

10 <sup>4</sup>Key Laboratory of Tibetan Environment Changes and Land Surface Processes, Institute of Tibetan Plateau Research, Chinese Academy of Sciences (CAS), Beijing, 100101, China

*Correspondence to: Chuanfeng Zhao (czhao@bnu.edu.cn)*

**Abstract.** To better understand the aerosol properties over the Arctic, Antarctic, and Tibetan Plateau (TP), the aerosol optical properties were investigated using 13 years CALIPSO L3 data, and the back  
15 trajectories for air masses were also simulated using the Hybrid Single Particle Lagrangian Integrated Trajectory (HYSPPLIT) model. The results show that the aerosol optical depth (AOD) has obvious spatial and seasonal variation characteristics, and the aerosol loading over Eurasia, Ross Sea, and South Asia is relatively large. The annual average AOD in the Arctic, Antarctic, and TP are 0.046, 0.025, and 0.098, respectively. The Arctic and Antarctic regions have larger AOD values in winter and spring,  
20 while the TP in spring and summer. There are no significant temporal trends of AOD anomalies in the three study regions. Clean marine and dust-related aerosols are the dominant types over ocean and land respectively in both the Arctic and Antarctic, while dust-related aerosol types have greater occurrence frequency (OF) over the TP. The OF of dust-related and elevated smoke is large for a broad range of heights, indicating that they are likely transported aerosols, while other types of aerosols mainly  
25 occurred at heights below 2 km in the Antarctic and Arctic. The maximum OF of dust-related aerosols mainly occurs at 6 km altitude over the TP. The analysis of back trajectories of the air masses shows large differences among different regions and seasons. The Arctic region is more vulnerable to mid-latitude pollutants than the Antarctic region, especially in winter and spring, while the air masses in the TP are mainly from the Iranian Plateau, Tarim Basin, and South Asia.



## 30 1 Introduction

As an important component, atmospheric aerosols play a crucial role in the Earth-atmosphere system (Garrett and Zhao, 2006; Ghan and Easter, 2006; Nabat et al., 2015). Aerosols have a variety of effects on Earth's climate, including the significant direct effect (Rap et al., 2013; Xing et al., 2017), indirect effect (Albrecht, 1989; Righi et al., 2011; Twomey, 1997; Zhao and Garrett, 2015), and semi-direct effect (Amiri-Farahani et al., 2017; Johnson, 2005; Koren et al., 2005). Meanwhile, different aerosol types often have different physical, chemical, and optical properties, and the balance between cooling and warming depends to some extent on aerosol characteristics (Boucher et al., 2013). The influence of aerosols on the Earth-atmosphere system depends on the vertical distribution of aerosols to a great extent (Kipling et al., 2016; McFarlane et al., 2007). The vertical distribution of aerosol is especially valuable as a signature of combined impacts, including the processes of aerosol emission, conversion, transport, and removal (Winker et al., 2013). Due to the lack of understanding of aerosol distribution, dynamics, and optical characteristics, the impact of aerosols on the global radiative budget in climate models has great uncertainty (Boucher et al., 2013; Loeb and Su, 2010). Thus, knowledge of aerosol characteristics is essential for determining the radiative forcing effects of aerosols, improving the accuracy of aerosol optical depth (AOD) retrieval using passive satellites, and quantifying the role of aerosols in global climate changes.

The acquisition of aerosol characteristics is mainly from two methods, ground-based monitoring and satellite remote sensing (Giles et al., 2012; Nishizawa et al., 2007; Omar et al., 2005; Russell et al., 2014). Ground-based remote sensing, such as the aerosol robotic network (AERONET), can provide high accuracy aerosol characteristics. The aerosol properties from AERONET are derived from direct sun extinction and sky radiance measurements, including columnar optical depth, single scattering albedo (SSA), Ångström exponent (AE), and so on (Lyamani et al., 2015; Ogunjobi et al., 2008). Although the aerosol characteristics can be obtained from ground-based remote sensing with high accuracy, they have some limitations in the study of global aerosol characteristics research. On one hand, it is difficult to acquire the vertical distributions of aerosols. On the other hand, due to the strong spatiotemporal variations of aerosols, the spatiotemporal representation of aerosol characteristics measured by ground stations is limited. Compared with passive satellite remote sensing, active satellite remote sensing, such as the Cloud-Aerosol Lidar with Orthogonal Polarization (CALIOP), can acquire



the vertical profile of the atmosphere and understand the vertical distribution of aerosol properties at a  
60 local or global scale (Shimizu et al., 2016). With three elastic backscattering channels, CALIOP is the  
first polarization lidar in space to provide three-dimensional atmospheric structure measurements  
(Granados-Muñoz et al., 2019; Peyridieu et al., 2010). It can measure the vertical distribution,  
microphysical, and optical properties of aerosols and clouds with a high vertical resolution at 1064 nm  
and a parallel and cross-polarized return signal at 532 nm (Kittaka et al., 2011; Kumar et al., 2016).  
65 CALIOP has high sensitivity and can detect weak aerosol layers with optical depths of 0.01 or less  
(Winker et al., 2007). The polarization measurements also allow the discrimination of spherical and  
non-spherical cloud and aerosol particles. Thus, CALIOP is widely used to the study of aerosol and  
cloud characteristics (Das and Jayaraman, 2011; Sun et al., 2018; Varnai and Marshak, 2010).

As two main cold sources of the global atmosphere, the Arctic and Antarctic play an irreplaceable key  
70 role in global climate change research. Located in the middle of Asia, the Tibetan Plateau (TP) is the  
largest ice sheet accumulation area except for the Arctic and Antarctic. The Arctic, Antarctic, and TP  
are representative of pristine regions, and they are very sensitive to global climate change (Lu et al.,  
2011). Associated with their different geographical environments, human activities have different  
effects on them. Previous studies have indicated that the clouds and radiation are particularly sensitive  
75 to aerosols over the pristine regions (Garrett and Zhao, 2006; Seinfeld et al., 2016; Wang et al., 2018).  
The Arctic, Antarctic, and TP have been undergoing unprecedented changes in global climate changes.

Extensive researches about aerosol properties over the pristine regions have been conducted (Di  
Carmine et al., 2005; Leaitch et al., 2020; Wu et al., 2018). The Arctic is a region with ample  
spatiotemporal variability in aerosols (Schmeisser et al., 2018). Due to the influence of pollutants  
80 transported (e.g. forest fire smoke, dust, soot, and sulfates) from lower latitudes, the AOD in the Arctic  
is abnormally high in winter and spring (Stone et al., 2014; Tomasi et al., 2007). While in the  
summertime, the oxidation of dimethyl sulfide (DMS), emitted by phytoplankton activity in the marine,  
can act as cloud condensation nuclei and exert significant control on sulfate aerosol (Leaitch et al.,  
2013). Meanwhile, by employing carbon monoxide as the assumed passive tracer, the relative  
85 contributions of transport efficiency and scavenging to seasonal variability of Arctic aerosol have also  
been evaluated (Garrett et al., 2010). In the past few decades, the aerosol properties in the Antarctic  
region, including their concentrations, size distribution, and chemical composition, have been



investigated mainly based on ground-based observations (Barbaro et al., 2017; Kerminen et al., 2000; Koponen et al., 2003). The aerosol properties of the Antarctic are mainly controlled by the Southern  
90 Ocean primary and secondary emissions and some periodical long-range transport (Asmi et al., 2018). Sea-salt coarse particle and sulfate fine particle aerosols are most abundant in the coastal Antarctic regions and over the Antarctic continental regions, respectively (Hall and Wolff, 1998; Wagenbach et al., 1998; Kerminen et al., 2000). Meanwhile, there are also obvious seasonal differences in Antarctic aerosol types. Sea salt and ammonium sulfate particles are dominant in the polar night months, while  
95 sulfuric acid droplets are the main particles in the sunlit months (Ito, 1985). The types of aerosols in the TP are complex, and the dominant aerosol type varies with site (Zhao et al., 2020). Dust aerosols in the northern parts of the TP and polluted aerosols over South Asia can reach internal regions of the TP through long-distance transport (Cong et al., 2015; Lüthi et al., 2015).

Although many studies have been carried out on aerosol optical properties over the Arctic, Antarctic,  
100 and TP, they are mainly based on the short-term ground remote sensing or in-situ observations, which has limited spatial representation (Chaubey et al., 2011; Cong et al., 2009; Eleftheriadis et al., 2004; Engvall et al., 2008; Pokharel et al., 2019), and inadequate information about the vertical distribution of aerosols. Meanwhile, different aerosol types can result in large uncertainty in estimating the aerosol radiative effect (Loeb and Su, 2010). Thus, it is essential to investigate the long-term aerosol  
105 characteristics over relatively large domains of the three pole regions, including the vertical profile information. In this study, the aerosol optical properties over the Arctic, Antarctic, and TP were investigated systematically, including the spatial and temporal distribution, vertical structure, and temporal trends of AOD and aerosol types. In addition, the back trajectory of air masses was also performed to determine the influence of ambient aerosols on the study areas.

## 110 2 Data and Methods

### 2.1 Study regions

As shown in Figure 1, the Arctic, Antarctic, and TP are selected as our study regions. The areas north of 65° N and south of 65° S are the study regions of the Arctic and Antarctic respectively, as shown in Figure 1 (a) and (b). The Arctic is an ocean covered by a thin layer of perennial sea ice and surrounded  
115 by land including Asia, Europe, and North America, while the Antarctic is dominated by the continent



covered by a very thick ice cap and surrounded by a rim of sea ice and the Southern Ocean. The TP is composed of land and ice sheets, and the surrounding environment is complex. As shown in Figure 1 (c), there are the Taklimakan Desert in the north and the heavily polluted South Asia in the south. Due to the coarse resolution of CALIPSO L3 data over the TP, the spatial and temporal distributions, as well as the temporal variation trends, were captured in a large region with latitudes from 25° to 41° N and longitudes from 65° to 105° E. However, the vertical characteristics of aerosol properties were only investigated in the inner region of the TP, which is marked by black dots as shown in Figure 1 (c). In addition, ten special locations (marked with green pentagrams) were selected for the study of aerosol sources using back trajectories, and the detailed information of ten sites can be found in Section 2.3 and Table S1.

## 2.2 CALIOP data

The CALIPSO satellite provides new sight into the role of how clouds and aerosols form, evolve, and affect weather and climate (Winker et al., 2007; 2010). Level 3 tropospheric aerosol profile product based on level 2 aerosol extinction profiles has the highest quality and is the most sophisticated among all CALIOP level 2 data products (Kim et al., 2018). Compared with the previous products, several changes in data quality screening have been made in the latest product to further avoid extinction retrieval errors, and the detailed algorithm has been depicted (Tackeett et al., 2018).

Compared with other sky conditions, the level 3 tropospheric cloud-free aerosol profile (NL3TCFAP) product has the highest quality as extinction retrievals are minimally affected by errors in retrieving the attenuation of overlying cloud cover (Tackett et al., 2018). Meanwhile, the NL3TCFAP product can describe in detail the near-global three-dimensional distribution of aerosols. Thus, to investigate the aerosol properties over three polar regions of the Arctic, Antarctic, and TP, the NL3TCFAP product including day and night time was used in this study. Up to now, the NL3TCFAP product contains seven types of aerosols, which are clean marine, dust, polluted continental/smoke, clean continental, polluted dust, elevated smoke, and dusty marine. The properties of different types of aerosols will be discussed in Section 3.2.

The NL3TCFAP product records aerosol properties data on a uniform 2° latitude by 5° longitude grid, and has a vertical resolution of 60 m for heights up to 12.1 km above mean sea level. In this study, the



mean AOD of each grid at different temporal scales was calculated, and the seasonal differences  
145 between the northern and southern hemispheres were also considered. In this study, the spring (autumn),  
summer (winter), autumn (spring), and winter (summer) are defined as March-May, June-August,  
September-November, and December-February in the north (south) hemisphere, respectively. Note that  
the aerosol properties in Figures 3, 4, and 7 over the TP region are only for the internal pixels of TP,  
which is marked by black dots in Figure 1 (c). In addition, the occurrence frequency (OF) of aerosol  
150 types was also calculated by counting the number of samples of seven aerosol types in each horizontal  
grid cell or altitude layer.

### 2.3 HYSPLIT model and GDAS data

The Hybrid Single-Particle Lagrangian Integrated Trajectory (HYSPLIT) model has been widely used  
in the simulation of atmospheric pollutant transport, dispersion, and deposition (Ashrafi et al., 2014;  
155 Jeong et al., 2012; Vernon et al., 2018; Zhao et al., 2009). To fully understand the sources of aerosols,  
the back trajectories of air masses at ten selected sites over three study regions mentioned above were  
examined using the latest version (V5.0.0) of the HYSPLIT model (Stein et al., 2015). Simultaneously,  
the multiple trajectories that are near each other were merged into groups through cluster analysis. In  
this study, the four Arctic sites are located in Greenland (N1), Northern Europe (N2), Northern Asia  
160 (N3), and Northern North American (N4). The four sites in the Antarctic are located on the Antarctic  
Peninsula (S1), Ross Sea (S2), Dronning Maud Land (S3), and Wilkes Land (S4). The two selected  
sites in the TP region are located on the northern (TP1) and southern (TP2) edges of the TP region. The  
locations of these sites are shown in Figure 1, and the detailed information of each site is shown in  
Table S1. Previous air mass back trajectory simulations in the Polar regions found that it is difficult to  
165 simulate the seasonal difference of the air mass with short-term back trajectory simulation, while the  
long-term back trajectory simulation has great uncertainties in the spatial domain (Hirdman et al., 2010;  
Sharma et al., 2013), thus a 14-day back trajectory simulation was adopted in this study (Rousseau et  
al., 2006), and the simulation date was set as the 15th and last day of each month which can help save a  
lot of computation sources while keeping the simulated back trajectories representative.



## 170 3 Results and Discussion

### 3.1 The spatial and temporal distribution of aerosol properties

#### 3.1.1 The spatial distribution of AOD

Figure 2 depicted the seasonal averaged spatial distribution of AOD over the Arctic, Antarctic, and TP, from which we can find that the AOD averaged between Jun 2006 and Dec 2019 has obvious spatial  
175 variation. In the Arctic, except for Greenland Island, aerosol loadings are larger over the continent than that over the ocean. On the contrary, aerosols loadings over the Antarctic continent are lower than that over the surrounding ocean. Aerosol loadings are found larger in the southern part of the Atlantic Ocean in the Antarctic, and decrease with the increase of latitude in any season. The aerosol concentration in the TP region is generally low while the aerosol loading in the regions around the TP  
180 (e.g. Tarim Basin in the north, Qaidam Basin in the northeast, Sichuan Basin in the east, and South Asia in the south) is large. In terms of regional differences, the aerosol concentration in the Arctic region is significantly higher than that in the Antarctic region. Meanwhile, the annual average AODs over the Arctic, Antarctic, and the inner region of the TP are 0.046, 0.025, and 0.098, respectively.

#### 3.1.2 The multi-year averaged seasonal variation of AOD

185 The aerosols and monsoon circulation patterns interact with each other (Ma and Guan, 2018), making it particularly valuable to know the seasonal variations of aerosol properties. In this study, we investigated the monthly variations of multi-year (June 2016 - December 2019) average AODs for three study regions. As shown in Figures 2 and 3, AOD has obvious seasonal variations, especially over the TP and Arctic, while the Antarctic AOD has relatively weak seasonal variation. The TP has a  
190 higher aerosol concentration in spring and summer, while high aerosol concentrations in the Arctic and Antarctic mainly occur in winter and spring. The north wind prevails over the TP region in spring, which makes the dust aerosols originating from the Tarim Basin and the Qaidam Basin have a greater contribution over the TP (Xu et al., 2015). And with the development of the South Asian monsoon and mid-latitude Westerlies, aerosols in South Asia are lifted under the influence of large-scale atmospheric  
195 circulation and cross the Himalayas to affect the internal region of the TP (Cong et al., 2015; Lüthi et al., 2015; Xia et al., 2011). The high aerosol concentration in the winter and spring Arctic is known as the Arctic haze phenomenon (Garrett and Zhao, 2006; Mitchell, 1957; Zhao and Garrett, 2015). On one



hand, anthropogenic aerosol from low and middle latitudes can disturb the Arctic atmosphere, especially from Eurasia. On the other hand, stable atmospheric status with less precipitation occurs in  
200 the Arctic winter, which makes it difficult for aerosols to be removed by wet deposition (Garrett et al., 2010; Heintzenberg, 1989). Among the three study regions, the AOD of the Antarctic is slightly higher than that of the Arctic in the southern hemisphere wintertime, while the AOD of the Antarctic is the lowest in other months. The slightly higher AOD shown in the Antarctic in spring and winter compared to the other two seasons may be due to a similar reason as in the Arctic: stable atmospheric conditions  
205 and less precipitation make the aerosols difficult to be removed in spring and winter.

### 3.1.3 The long-term trend of AOD

To study the long-term trend of AOD over the Arctic, Antarctic, and TP, the monthly AODs along with their standard deviations from June 2007 to December 2019 were calculated using valid data in the study areas. In order to remove the clear seasonal variation of AOD as found earlier in the study  
210 regions, the deseasonalized trend was carried out by calculating the AOD anomalies. The AOD anomaly here is defined as the difference between the monthly average value of AOD in each month and the average value of AOD for that month in all years. The results of the monthly AOD anomaly over the Arctic, Antarctic, and TP are outlined in Figure 4. The solid line with red color represents the monthly AOD anomaly, the shadow region represents the single standard deviations, and the blue  
215 dotted line represents the linear trend based on deseasonalized monthly AOD anomalies from June 2006 to December 2019. Figure 4 shows that there are no significant increasing or decreasing trends of AOD anomalies in the Arctic, Antarctic, and TP (slope =  $-0.00724\%$  ~  $-0.00219\%$ ), although the linear trends show a high confidence level ( $p > 0.05$ ). It is worth noting that the deseasonalized monthly AOD anomalies over the TP region are relatively high. There are two likely reasons. First, there are  
220 anthropogenic emission sources over the TP region. Second, the TP is located in Central Asia surrounded by highly polluted areas, which is easily affected by external aerosol transport.

## 3.2 The properties of different aerosol types

### 3.2.1 Horizontal distribution

In order to examine the spatial and temporal variability of aerosol types, the normalized annual and  
225 seasonal averaged OFs of different aerosol types over the (a) Arctic, (b) Antarctic, and (c) TP were





presented in Figure 5 and Table 1, respectively. The number i ~ vii represent OF of clean marine, dust, polluted continental/smoke, clean continental, polluted dust, elevated smoke, and dusty marine aerosol, respectively.

In terms of the spatial distribution of aerosol OF among the three study regions, it can be seen from  
230 Figure 5 that the annual average OF of aerosol types is roughly similar in both the Arctic and Antarctic.  
The dominant aerosol type is the clean marine, followed by polluted continental/smoke and polluted  
dust. The annual average proportion of time with clean marine aerosol dominant in the Arctic and  
Antarctic is about 32.8% and 37.5%, respectively. In contrast, the dominant aerosol types over the TP  
are dust type and polluted dust type, which show the dominant role for 92% time of the whole year.  
235 Figure 5 also shows that there are large differences in the spatial distribution of different aerosol types  
over all study regions. However, the spatial distribution of aerosol types has a distinctive feature, that is,  
the OFs of dust (ii), polluted continental/smoke (iii), and polluted dust (v) over the land are  
significantly higher than that over the ocean area in the Arctic and Antarctic. The clean marine (i)  
aerosol mainly occurs in the sea area of the Arctic and Antarctic regions, and the farther away from the  
240 land, the higher the OF of clean marine aerosol. Clean continental (iv) aerosol only occurs in the land  
area, while dusty marine aerosol (vii) only occurs in the marine area. The OF of elevated smoke (vi)  
does not differ significantly between land and sea areas, which can be explained to a certain extent by  
the fact that the elevated smoke aerosols in the Antarctic and Arctic are mainly transported from the  
outside.

245 There is also a significant difference in the OF spatial distribution of different aerosol types in each  
study region. In the Arctic, dust (ii) and polluted dust (v) aerosol has a higher frequency of occurrence  
over the Greenland, northeastern Asia, and northern America due to the transport of Asian dust into the  
atmosphere, which was subsequently transported eastward and reached the high-latitude regions of  
Northern America (Tomasi et al., 2007; VanCuren et al., 2012). In contrast, polluted continental/smoke  
250 (iii) aerosol mainly occurs in Eurasia, which is mainly due to biomass burning (e.g., agricultural  
burning and wildfires) in the Eurasian region (Soja et al., 2006; Warneke et al., 2010). In the Antarctic,  
there are obvious spatial differences in aerosol types. Specifically, dust (ii) and polluted dust (v)  
aerosols are the dominant aerosol types that occurred in East Antarctica. The main aerosol type in  
Western Antarctic (Antarctic Peninsula) is polluted continental/smoke (iii) aerosols, but there is also a



255 certain proportion of polluted dust (v) aerosol in West Antarctica, similar to the findings reported by Li  
et al. (2008). The clean marine aerosol mainly occurs in the Southern Ocean and decreases drastically  
in the interior of Antarctica in occurrence frequency (Teinilä et al., 2014; Virkkula et al., 2006). For the  
TP region, dust aerosols occur more frequently in the north and west of the TP, which is mainly  
because they are close to desert source areas, including Taklimakan Desert, Qaidam Basin, and Iranian  
260 Plateau. Differently, the polluted dust in the south of the TP has a higher frequency of occurrence,  
which may be due to the impact of South Asia anthropogenic pollutants and biomass burning aerosols.  
Similarly, polluted continental/smoke and elevated smoke also have a higher frequency in the southern  
TP.

As mentioned above, aerosol types have a distinct seasonal variation. We then investigated the seasonal  
265 average OF of different aerosol types. In this study, the number of samples of seven aerosol types in  
each study region was first counted, and then the normalized OF of different aerosol types was  
calculated seasonally. Similar to the findings in Figure 5, in general, the dominated aerosol type is  
clean marine over the Arctic and Antarctic. However, the normalized OF of aerosol types display a  
substantial seasonal dependence (Table 1). Specifically, the proportion of clean marine aerosols is  
270 larger in the Arctic in autumn and winter than that in spring and summer. This may be due to the wind  
speed in winter half-year in the Arctic region is higher than that in summer half-year, which makes  
more marine aerosols enter the atmosphere (Erickson et al., 1986). In the summer fire season, the  
wildfires and agricultural burning occur more frequently over Siberian and North American, which can  
be transported to the Arctic along with the pollutants, resulting in a high proportion of polluted  
275 continental/smoke aerosol and elevated smoke aerosol. This notion is also supported by previous  
studies (Stohl et al., 2006; Schmeisser et al., 2018; Tomasi et al., 2007). In spring, meanwhile, the  
proportion of dust and polluted dust increases significantly in the Arctic, which is due to the  
transported dust from Asian desert sources (Barrie, 1995). Different from the Arctic, clean marine  
aerosol was the dominant aerosol type in the Antarctic, especially in summer, accounting for about 61.2  
280 %. Similar results were reported by Quinn et al. (1998). Meanwhile, there is a high proportion of dust  
aerosols in the Antarctic except in winter. It is also found that polluted continental/smoke aerosol in the  
southern hemisphere in winter and spring has a relatively large proportion, consistent well with  
previous findings that there is more equivalent back carbon concentrations in spring and winter than



that in summer and autumn (Bodhaine, 1995; Weller et al., 2013). Compared with the Antarctic and  
285 Arctic regions, the types of aerosols in the TP are relatively simple, which are mainly the dust aerosol  
and polluted dust aerosol. In spring and summer, the proportion of dust aerosol is relatively high, which  
is due to the northerly jet over the TP carrying dust aerosols to the internal TP. In autumn and winter,  
the emission of anthropogenic aerosol increases, and the proportion of mixed anthropogenic aerosol  
and dust aerosol increases continuously over the TP. In addition, the OF of polluted continental/smoke  
290 aerosol in winter is much higher than that in other seasons, which may be due to the increase of  
biomass combustion.

### 3.2.2 The vertical extinction coefficient of dominant aerosol type

Knowledge of aerosol extinction coefficient is necessary to enhance our understanding of how  
atmospheric aerosols impact the weather and climate to a certain extent (Jung et al., 2019). The  
295 extinction properties of the three typical aerosol types (including dust, elevated smoke, and polluted  
dust) and the average value of the extinction of all aerosol types were retrieved in the CALIPSO L3  
aerosol profile product. In this study, the seasonal average aerosol extinction coefficient profiles  
(Spring: (a) ~ (c); Summer: (d) ~ (f); Autumn: (g) ~ (i); Winter: (j) ~ (l)) over the Arctic, Antarctic, and  
TP were calculated statistically and shown in Figure 6.

300 As Figure 6 shows, there is no doubt that the aerosol extinction coefficient profile has a significant  
regional difference. In general, the aerosol extinction coefficient in the Arctic has a broad vertical  
distribution at heights ranging from 0 to 12 km, but the vertical distribution of the Antarctic aerosol  
extinction coefficient is uneven. In the Antarctic, the extinction layer can reach a maximum height at  
11 km in winter (k) and spring (b), while it is mainly distributed below 5 km in summer (e) and autumn  
305 (h). The vertical distribution of aerosols over the TP is more concentrated, with most aerosols  
distributed between 2 and 8 km. The vertical distribution of extinction coefficients of different aerosol  
types also demonstrates large regional differences. The elevated smoke in the Arctic has a larger  
extinction coefficient when the altitude is greater than 2 km, especially in summer (d) and autumn (g);  
while in the near-ground area (altitude < 2 km), dust and polluted dust have a larger extinction  
310 coefficient, which is in good agreement with previous studies (Di Biagio et al., 2018). The extinction  
coefficients of aerosols in the Antarctic have obvious seasonal characteristics. The vertical distribution  
patterns of extinction coefficients for the three aerosol types in spring (b) and autumn (h) are basically



the same, and the extinction layers are mainly concentrated at heights below 5 km. In summer (e), the vertical distributions of extinction coefficients are quite different among the different types of aerosols.

315 The elevated smoke is mainly concentrated at heights about 3 km, while the dust-related aerosol types are more distributed at heights below 2 km. In winter (k), on the contrary, the extinction coefficient of dust and elevated smoke increases significantly above 5 km, and the polluted dust aerosols have large extinction coefficients under 5 km. Unlike the Arctic and Antarctic regions, the extinction coefficients of smoke and dust-related aerosols over the TP region are larger at heights of 4 - 9 km and 2 - 9 km,

320 respectively. From the perspective of seasonal variation, the vertical distribution of dust-related aerosol extinction coefficient is larger in spring (c) and summer (f) than in autumn (i) and winter (l). These vertical distribution information can help better understand the sources and impacts of aerosols over the three study regions in future. For example, aerosol information below clouds could be particularly important for aerosol-cloud interaction study.

### 325 **3.2.3 Vertical distribution**

Aerosol types not only have significant spatial and temporal variations, but also vary with height. CALIPSO data provides the vertical distribution of aerosol types at 208 levels, ranging from surface to 12 km. We here investigate the vertical distribution of seven aerosol types, as shown in Figure 7. The results show that most of the aerosol types in the Arctic and Antarctic regions have similar vertical

330 distribution patterns, except for dust and polluted dust. Clean marine, polluted continental/smoke, clean continental, and dusty marine mainly occur near the surface with altitudes below 3 km. Different from the above aerosol types, the highest OF of elevated smoke occurs at a height of about 2.5 km, and occurs at 8 km and 4 km, respectively in the Arctic and Antarctic regions, which indicates that the main source of elevated smoke is external transport. In addition, polluted continental/smoke aerosols occur

335 more frequently in the Arctic region than in the Antarctic region. This is mainly due to the fact that the Arctic region is surrounded by more continents and more continental pollutants can enter the Arctic region. Compared with the Arctic, the dust and polluted dust in the Antarctic region have obvious vertical distribution characteristics. The dust and polluted dust aerosols are mainly located within 3 - 5 km in the Antarctic, which indicates that the dust-related aerosols in the Antarctic area are mainly

340 transported from outside through the upper air (Li et al., 2008). Similar to previous studies, dust-related



aerosol layers over the TP appear most frequently at approximately 4 - 7 km above the mean sea level, where the plumes likely originate from the nearby Taklimakan Desert (Huang et al., 2007).

### 3.3 Back trajectory

In order to better understand the origins of the air masses arriving in the study regions, the latest  
345 version (V5.0.0) of the HYSPLIT model was used in this study to simulate the back trajectories of air masses. Ten sites listed in Table S1 were selected in this study, and the 14-day back trajectories for the Arctic, Antarctic, and TP sites were simulated. A total of 3,120 ( $10 \times 2 \times 12 \times 13$ ) back trajectories were computed at a height of 500 m above the surface at all ten sites. The seasonal climatologies (January 2007 ~ December 2019) of air mass trajectories were created and the cluster analysis was implemented  
350 to examine the long-range transport pathways of air masses. The cluster analysis determines the final number of clusters based on the total spatial variance (Draxler and Hess, 1998). Figure 8 reveals the seasonal climatological characteristics of the back trajectories after cluster analysis. It can be seen that the back trajectories over different study regions have distinctive characteristics, especially in the TP region. Compared with the Antarctic, the air mass trajectory in the Arctic region has a shorter transport  
355 distance. This is most likely due to the fact that the temperature in the Arctic is higher than that in the Antarctic, which decreases the pressure gradient and reduces the wind speed. In the Arctic, the difference of back trajectories between summer and winter half-year is obvious, with more proportion of air masses from the Eurasian in winter and spring. At the same time, Asian dust storms prevail in spring, resulting in a greater proportion of dust and polluted dust in spring. In contrast, the influence of  
360 external transport of aerosols is relatively small in autumn, and the larger wind speed allows more marine aerosols enter the atmosphere, which together make the contribution of clean marine aerosols in autumn relatively large in the Arctic.

In the Antarctic region, the seasonal difference in air mass trajectories is relatively small compared with the Arctic region, and the air mass trajectories were mainly controlled by circumpolar westerly  
365 winds (Ravi et al., 2011). While it is not clearly shown by the air mass back trajectory simulation results, dust and polluted dust over East Antarctica was likely caused by the transport from South America and Africa, and the polluted dust over West Antarctica was more likely affected by the aerosol transport from South America and Australia. Generally speaking, under the influence of steady and



strong westerly winds, dust and carbonaceous aerosols in South America, Australia, and Africa have a  
370 certain impact on Antarctic pollution (Li et al., 2018; McConnell et al., 2007; Zou et al., 2018).

Different from the Arctic and Antarctic, the back trajectories of air masses over the TP have significant  
seasonal variation. In spring and summer, the air masses located on the northern slope of TP mainly  
come from the northern desert area. In autumn, the air masses from the north begin to weaken, while  
the air masses from Iranian Plateau begin to increase and reach the maximum in winter (93.15 %). For  
375 the station on the southern slope of the TP, the air masses mainly come from the Iranian Plateau in  
spring and winter, while in summer they mainly come from South Asia, which causes more biomass  
burning aerosols to enter the TP.

#### 4 Summary and Conclusions

Aerosols play a crucial role in the radiative budget of the Earth-atmosphere system, but due to  
380 insufficient understanding of aerosol properties, at least partly, the uncertainty of the total radiative  
forcing by aerosols in the climate mode is still the largest. Understanding the properties of aerosols is  
highly demanded. The satellite active remote sensing can make up for the insufficiency of  
ground-based remote sensing to obtain long-term and large-scale aerosol properties. In this study, the  
spatial and temporal distribution of the aerosol optical depth (AOD) and aerosol type over the Arctic,  
385 Antarctic, and Tibetan Plateau (TP) regions were investigated. In addition, ten typical sites were  
selected and the back trajectories of air masses were simulated using the Hybrid Single-Particle  
Lagrangian Integrated Trajectory (HYSPPLIT) model. The main findings are as follows.

The distribution of AOD over the three study regions shows distinctive spatial and seasonal differences.  
In general, the AOD over the Arctic and Antarctic decreases with the increasing latitude. In the Arctic,  
390 the AOD over land is greater than that over the ocean, while the opposite is true for the Antarctic.  
Eurasia and the Ross Sea are the high AOD areas in the Arctic and Antarctic, respectively. The annual  
average of AOD over the TP region (0.098) is about twice that of the Arctic (0.046) and four times that  
of the Antarctic (0.025). The seasonal variation of AOD over the TP is the most distinctive due to the  
influence of transported aerosols from surrounding high emission regions. The maximum AOD occurs  
395 in spring and summer over the TP, while occurs in winter and spring over the Arctic and Antarctic  
regions.



The deseasonalized trend of AOD (called AOD anomaly) over the three regions was also investigated. The result shows that there were no obvious temporal trends in the AOD anomalies over the Arctic, Antarctic, and TP. Compared with the Antarctic and Arctic, the AOD anomalies over the TP have  
400 obvious fluctuations, which indicates that the TP is more susceptible to the influence of highly varied aerosols from different regions. In the Arctic, the aerosol extinction coefficient has a broad vertical distribution at heights from the surface to 12 km. Moreover, the extinction coefficient of elevated smoke and polluted dust in the upper layer is large in the Arctic, especially in summer and autumn. In the Antarctic, the vertical distribution of aerosol extinction has obvious seasonal differences. Dust  
405 aerosol has a large extinction coefficient at heights 5 - 11 km in winter, while in other seasons, the aerosol extinction coefficient is large at heights below 5 km.

The multi-year average (June 2006 ~ December 2019) occurrence frequency (OF) of aerosol types was also examined. The OF of different aerosol types demonstrates significant spatial differences. In the Antarctic and Arctic regions, the dominant aerosol type is the clean marine type, followed by polluted  
410 continental/smoke and polluted dust aerosol types. Clean marine aerosol types are mainly distributed over the seas of the polar regions, and polluted continental/smoke and polluted dust are mainly distributed over the land regions. In the Arctic, polluted continental/smoke aerosol types are mainly distributed in the northern part of Europe, while polluted dust aerosols are widely distributed in the northern parts of Asia and America along with the Greenland Island region. In the Antarctic, dust and  
415 polluted dust aerosol types are mainly distributed in East Antarctica, and polluted continental/smoke aerosol types are mainly distributed in the Antarctic Peninsula. In the TP region, the main aerosol types in the north and south of the TP are dust and polluted dust, respectively. The normalized seasonal OF of seven aerosol types is further investigated. The result shows that the OF of each aerosol type in different regions has obvious seasonal variations. Regarding the vertical distribution of the OF of  
420 aerosol types, dust, polluted dust, and elevated smoke have a relatively large OF at higher altitudes. And the maximum altitude with a noticeable OF of these types of aerosols is higher in the Antarctic than in the Arctic. Different from the Arctic and Antarctic, the dust-related aerosol layers over the TP appear most frequently at heights approximately 4 - 7 km above the mean sea level.

The back trajectories of air masses indicate that the Arctic region is vulnerable to mid-latitude  
425 pollutants, especially in winter and spring, while the Antarctic region is less affected by the



mid-latitude pollutants. Different from that in the Arctic and Antarctic, the air mass trajectories over the TP have obvious seasonal variations.

#### **Data Availability.**

The CALIPSO dataset were obtained from <https://earthdata.nasa.gov/>. Surface elevation data from Shuttle Radar Topography Mission (SRTM) were downloaded from <http://srtm.csi.cgiar.org/>. HYSPLIT data are provided by the NOAA READY website (<http://www.ready.noaa.gov>).

#### **Acknowledgement.**

This research was supported by the Strategic Priority Research Program of the Chinese Academy of Sciences (Grant number XDA19070202), the Natural Science Foundation of China (41925022, 91837204). The authors gratefully acknowledge the data support from NASA for making CALIPSO L3 datasets accessible in public. We also gratefully thank the NOAA Air Resources Laboratory (ARL) for the provision of the HYSPLIT transport and dispersion model. We thank the reviewers of this paper for their valuable comments which helped improve the manuscript.

#### **Author contributions.**

CFZ designed the research, and CFZ and YKY carried out the research and wrote the manuscript. QW and XCY contributed to run the HYSPLIT model. ZYC and HF provided constructive comments on this research. CFZ, ZYC, and YKY revised the manuscript. All authors made substantial contributions to this work.

#### **Competing interests.**

The authors declare that they have no conflict of interest.

#### **References.**

Albrecht, B.: Aerosols, cloud microphysics, and fractional cloudiness, *Science*, 245, 1227-1230, 10.1126/science.245.4923.1227, 1989.





- Amiri-Farahani, A., Allen, R., Neubauer, D., and Lohmann, U.: Impact of Saharan dust on North  
450 Atlantic marine stratocumulus clouds: importance of the semidirect effect, *Atmospheric Chemistry and  
Physics*, 17, 6305-6322, 10.5194/acp-17-6305-2017, 2017.
- Ashrafi, K., Shafiepour-Motlagh, M., Aslemand, A., and Ghader, S.: Dust storm simulation over Iran  
using HYSPLIT, *Journal of Environmental Health Science and Engineering*, 12,  
10.1186/2052-336x-12-9, 2014.
- 455 Asmi, E., Neitola, K., Teinila, K., Rodriguez, E., Virkkula, A., Backman, J., Bloss, M., Jokela, J.,  
Lihavainen, H., De Leeuw, G., Paatero, J., Aaltonen, V., Mei, M., Gambarte, G., Copes, G., Albertini,  
M., Perez Fogwill, G., Ferrara, J., Elena Barlasina, M., and Sanchez, R.: Primary sources control the  
variability of aerosol optical properties in the Antarctic Peninsula, *Tellus Series B-Chemical and  
Physical Meteorology*, 70, 10.1080/16000889.2017.1414571, 2018.
- 460 Barbaro, E., Padoan, S., Kirchgeorg, T., Zangrando, R., Toscano, G., Barbante, C., and Gambaro, A.:  
Particle size distribution of inorganic and organic ions in coastal and inland Antarctic aerosol,  
*Environmental Science and Pollution Research*, 24, 2724-2733, 10.1007/s11356-016-8042-x, 2017.
- Barrie L.: Arctic Aerosols: Composition, Sources and Transport. In: Delmas R.J. (eds) *Ice Core Studies  
of Global Biogeochemical Cycles. NATO ASI Series (Series I: Global Environmental Change)*, vol 30.  
465 Springer, Berlin, Heidelberg. 10.1007/978-3-642-51172-1\_1, 1995.
- Bodhaine, B.: Aerosol absorption measurements at Barrow, Mauna Loa and the South Pole, *Journal of  
Geophysical Research-Atmosphere*, 100, 8967-8975, 10.1029/95JD00513, 1995.
- Boucher, O., Randall, D., Artaxo, P., Bretherton, C., Feingold, G., Forster, P., Kerminen, V.-M., Kondo,  
Y., Liao, H., Lohmann, U., Rasch, P., Satheesh, S., Sherwood, S., Stevens, B., and Zhang, X.: Clouds  
470 and Aerosols. In: *Climate Change 2013: The Physical Science Basis. Contribution of Working Group I  
to the Fifth Assessment Report of the Intergovernmental Panel on Climate Change [Stocker, T., D. Qin,  
G.-K. Plattner, M. Tignor, S. Allen, J. Boschung, A. Nauels, Y. Xia, V. Bex and P. Midgley (eds.)]*.  
Cambridge University Press, Cambridge, United Kingdom and New York, NY, USA. 2013.
- Chaubey, J., Moorthy, K., Babu, S., and Nair, V.: The optical and physical properties of atmospheric  
475 aerosols over the Indian Antarctic stations during southern hemispheric summer of the International  
Polar Year 2007-2008, *Annales Geophysicae*, 29, 109-121, 10.5194/angeo-29-109-2011, 2011.



- Cong, Z., Kang, S., Kawamura, K., Liu, B., Wan, X., Wang, Z., Gao, S., and Fu, P.: Carbonaceous aerosols on the south edge of the Tibetan Plateau: concentrations, seasonality and sources, *Atmospheric Chemistry and Physics*, 15, 1573-1584, 10.5194/acp-15-1573-2015, 2015.
- 480 Cong, Z., Kang, S., Smirnov, A., and Holben, B.: Aerosol optical properties at Nam Co, a remote site in central Tibetan Plateau, *Atmospheric Research*, 92, 42-48, 10.1016/j.atmosres.2008.08.005, 2009.
- Das, S., and Jayaraman, A.: Role of black carbon in aerosol properties and radiative forcing over western India during premonsoon period, *Atmospheric Research*, 102, 320-334, 10.1016/j.atmosres.2011.08.003, 2011.
- 485 Di Biagio, C., Pelon, J., Ancellet, G., Bazureau, A., and Mariage, V.: Sources, Load, Vertical Distribution, and Fate of Wintertime Aerosols North of Svalbard From Combined V4 CALIOP Data, Ground-Based IAOS Lidar Observations and Trajectory Analysis, *Journal of Geophysical Research-Atmospheres*, 123, 1363-1383, 10.1002/2017jd027530, 2018.
- Di Carmine, C., Campanelli, M., Nakajima, T., Tomasi, C., and Vitale, V.: Retrievals of Antarctic aerosol characteristics using a Sun-sky radiometer during the 2001-2002 austral summer campaign, 490 *Journal of Geophysical Research-Atmospheres*, 110, 10.1029/2004jd005280, 2005.
- Draxier, R., and Hess, G.: An overview of the HYSPLIT\_4 modelling system for trajectories, dispersion and deposition, *Australian Meteorological Magazine*, 47, 295-308, 1998.
- Eleftheriadis, K., Nyeki, S., Psomiadou, C., and Colbeck, I.: Background aerosol properties in the 495 European Arctic, *Protection and Restoration of the Environment VI*, Vols I - Iii, Proceedings, edited by: Kungolos, A. G., Liakopoulos, A. B., Korfiatis, G., Koutsospyros, A. D., Katsifarakis, K. L., and Demetracopoulos, A. D., 999-1004 pp., 2002.
- Engvall, A., Krejci, R., Strom, J., Treffeisen, R., Scheele, R., Hermansen, O., and Paatero, J.: Changes in aerosol properties during spring-summer period in the Arctic troposphere, *Atmospheric Chemistry and Physics*, 8, 445-462, 10.5194/acp-8-445-2008, 2008.
- 500 Erickson, D. J., Merrill, J. T., and Duce, R. A.: Seasonal Estimates of Global Atmospheric Sea-Salt Distribution, *Journal of Geophysical Research-Atmospheres*, 91, 1067-1072, 10.1029/JD091iD01p01067, 1986.



- Garrett, T., and Zhao, C.: Increased Arctic cloud longwave emissivity associated with pollution from  
505 mid-latitudes, *Nature*, 440, 787-789, 10.1038/nature04636, 2006.
- Garrett, T., Zhao, C., and Novelli, P.: Assessing the relative contributions of transport efficiency and  
scavenging to seasonal variability in Arctic aerosol, *Tellus Series B-Chemical and Physical  
Meteorology*, 62, 190-196, 10.1111/j.1600-0889.2010.00453.x, 2010.
- Ghan, S., and Easter, R.: Impact of cloud-borne aerosol representation on aerosol direct and indirect  
510 effects, *Atmospheric Chemistry and Physics*, 6, 4163-4174, 10.5194/acp-6-4163-2006, 2006.
- Giles, D., Holben, B., Eck, T., Sinyuk, A., Smirnov, A., Slutsker, I., Dickerson, R. R., Thompson, A.  
M., and Schafer, J. S.: An analysis of AERONET aerosol absorption properties and classifications  
representative of aerosol source regions, *Journal of Geophysical Research-Atmospheres*, 117,  
10.1029/2012jd018127, 2012.
- 515 Granados-Muñoz, M., Sicard, M., Papagiannopoulos, N., Barragan, R., Antonio Bravo-Aranda, J., and  
Nicolae, D.: Two-dimensional mineral dust radiative effect calculations from CALIPSO observations  
over Europe, *Atmospheric Chemistry and Physics*, 19, 13157-13173, 10.5194/acp-19-13157-2019,  
2019.
- Hall, J., and Wolff, E.: Causes of seasonal and daily variations in aerosol sea-salt concentrations at a  
520 coastal Antarctic station, *Atmospheric Environment*, 32, 3669-3677, 10.1016/s1352-2310(98)00090-9,  
1998.
- Heintzenberg, J.: Arctic haze-air-pollution in polar-regions, *Ambio*, 18, 50-55, 1989.
- Hirdman, D., Burkhardt, J., Sodemann, H., Eckhardt, S., Jefferson, A., Quinn, P., Sharma, S., Strom, J.,  
and Stohl, A.: Long-term trends of black carbon and sulphate aerosol in the Arctic: changes in  
525 atmospheric transport and source region emissions, *Atmospheric Chemistry and Physics*, 10,  
9351-9368, 10.5194/acp-10-9351-2010, 2010.
- Huang, J., Minnis, P., Yi, Y., Tang, Q., Wang, X., Hu, Y., Liu, Z., Ayers, K., Trepte, C., and Winker,  
D.: Summer dust aerosols detected from CALIPSO over the Tibetan Plateau, *Geophysical Research  
Letters*, 34, 10.1029/2007gl029938, 2007.
- 530 Ito, T.: Study of background aerosols in the Antarctic troposphere, *Journal of Atmospheric Chemistry*,  
3, 69-91, 10.1007/bf00049369, 1985.



- Jeong, S., Zhao, C., Andrews, A., Dlugokencky, E., Sweeney, C., Bianco, L., Wilczak, J., and Fischer, M.: Seasonal variations in N<sub>2</sub>O emissions from central California, *Geophysical Research Letters*, 39, 10.1029/2012gl052307, 2012.
- 535 Johnson, B.: The semidirect aerosol effect: Comparison of a single-column model with large eddy simulation for marine stratocumulus, *Journal of Climate*, 18, 119-130, 10.1175/jcli-3233.1, 2005.
- Jung, C., Lee, J., Um, J., Lee, S., Yoon, Y., and Kim, Y.: Estimation of Source-Based Aerosol Optical Properties for Polydisperse Aerosols from Receptor Models, *Applied Sciences-Basel*, 9, 10.3390/app9071443, 2019.
- 540 Kerminen, V., Teinila, K., and Hillamo, R.: Chemistry of sea-salt particles in the summer Antarctic atmosphere, *Atmospheric Environment*, 34, 2817-2825, 10.1016/s1352-2310(00)00089-3, 2000.
- Kim, M., Omar, A., Tackett, J., Vaughan, M., Winker, D., Trepte, C., Hu, Y., Liu, Z., Poole, L., Pitts, M., Kar, J., and Magill, B.: The CALIPSO Version 4 Automated Aerosol Classification and Lidar Ratio Selection Algorithm, *Atmospheric Measurement Techniques*, 11, 6107-6135, 545 10.5194/amt-11-6107-2018, 2018.
- Kipling, Z., Stier, P., Johnson, C., Mann, G., Bellouin, N., Bauer, S., Bergman, T., Chin, M., Diehl, T., Ghan, S., Iversen, T., Kirkevåg, A., Kokkola, H., Liu, X., Luo, G., van Noije, T., Pringle, K., von Salzen, K., Schulz, M., Seland, O., Skeie, R., Takemura, T., Tsigaridis, K., and Zhang, K.: What controls the vertical distribution of aerosol? Relationships between process sensitivity in 550 HadGEM3-UKCA and inter-model variation from AeroCom Phase II, *Atmospheric Chemistry and Physics*, 16, 2221-2241, 10.5194/acp-16-2221-2016, 2016.
- Kittaka, C., Winker, D., Vaughan, M., Omar, A., and Remer, L.: Intercomparison of column aerosol optical depths from CALIPSO and MODIS-Aqua, *Atmospheric Measurement Techniques*, 4, 131-141, 10.5194/amt-4-131-2011, 2011.
- 555 Koponen, I., Virkkula, A., Hillamo, R., Kerminen, V., and Kulmala, M.: Number size distributions and concentrations of the continental summer aerosols in Queen Maud Land, Antarctica, *Journal of Geophysical Research-Atmospheres*, 108, 10.1029/2003jd003614, 2003.
- Koren, I., Kaufman, Y., Remer, L., and Martins, J.: Measurement of the effect of Amazon smoke on inhibition of cloud formation, *Science*, 303, 1342-1345, 10.1126/science.1089424, 2004.



- 560 Kumar, M., Singh, R., Murari, V., Singh, A., Singh, R., and Banerjee, T.: Fireworks induced particle pollution: A spatio-temporal analysis, *Atmospheric Research*, 180, 78-91, 10.1016/j.atmosres.2016.05.014, 2016.
- Leaitch, W., Kodros, J., Willis, M., Hanna, S., Schulz, H., Andrews, E., Bozem, H., Burkart, J., Hoor, P., Kolonjari, F., Ogren, J., Sharma, S., Si, M., von Salzen, K., Bertram, A., Herber, A., Abbatt, J., and  
565 Pierce, J.: Vertical profiles of light absorption and scattering associated with black carbon particle fractions in the springtime Arctic above 79° N, *Atmospheric Chemistry and Physics*, 20, 10545-10563, 10.5194/acp-20-10545-2020, 2020.
- Leaitch, W., Sharma, S., Huang, L., Toom-Sauntry, D., Chivulescu, A., Macdonald, A., von Salzen, K., Pierce, J., Bertram, A., Schroder, J., Shantz, N., Chang, R., and Norman, A.: Dimethyl sulfide control of  
570 the clean summertime Arctic aerosol and cloud, *Elementa*, 1, 000017, <https://doi.org/10.12952/journal.elementa.000017>, 2013.
- Li, F., Ginoux, P., and Ramaswamy, V.: Distribution, transport, and deposition of mineral dust in the Southern Ocean and Antarctica: Contribution of major sources, *Journal of Geophysical Research-Atmospheres*, 113, 10.1029/2007jd009190, 2008.
- 575 Loeb, N., and Su, W.: Direct Aerosol Radiative Forcing Uncertainty Based on a Radiative Perturbation Analysis, *Journal of Climate*, 23, 5288-5293, 10.1175/2010jcli3543.1, 2010.
- Lu, L., Bian, L., and Zhang, Z.: Climate change: Impact on the Arctic, Antarctic and Tibetan Plateau, *Advances in Polar Science*, 22, 67-73, 10.3724/SP.J.1085.2011.00067, 2011.
- Lüthi, Z., Skerlak, B., Kim, S., Lauer, A., Mues, A., Rupakheti, M., and Kang, S.: Atmospheric brown  
580 clouds reach the Tibetan Plateau by crossing the Himalayas, *Atmospheric Chemistry and Physics*, 15, 6007-6021, 10.5194/acp-15-6007-2015, 2015.
- Lyamani, H., Valenzuela, A., Perez-Ramirez, D., Toledano, C., Granados-Munoz, M., Olmo, F., and Alados-Arboledas, L.: Aerosol properties over the western Mediterranean basin: temporal and spatial variability, *Atmospheric Chemistry and Physics*, 15, 2473-2486, 10.5194/acp-15-2473-2015, 2015.
- 585 Ma, F., and Guan, Z.: Seasonal Variations of Aerosol Optical Depth over East China and India in Relationship to the Asian Monsoon Circulation, *Journal of Meteorological Research*, 32, 648-660, 10.1007/s13351-018-7171-1, 2018.



- 590 McConnell, J., Aristarain, A., Banta, J., Edwards, P., and Simoes, J.: 20th-Century doubling in dust archived in an Antarctic Peninsula ice core parallels climate change and desertification in South America, *Proceedings of the National Academy of Sciences of the United States of America*, 104, 5743-5748, 10.1073/pnas.0607657104, 2007.
- McFarlane, S., Kassianov, E., and Flynn, C., 2007. Vertical profiles of aerosol extinction and radiative heating at Niamey, Niger. American Geophysical Union, Fall Meeting 2007, abstract id. A41A-0013.
- Mitchell, J.: Visual range in the polar regions with particulate reference to the Alaskan Arctic, *J. Atmos. Terr. Phys.*, special supplement, 195–211, 1957.
- 595 Nabat, P., Somot, S., Mallet, M., Sevault, F., Chiacchio, M., and Wild, M.: Direct and semi-direct aerosol radiative effect on the Mediterranean climate variability using a coupled regional climate system model, *Climate Dynamics*, 44, 1127-1155, 10.1007/s00382-014-2205-6, 2015.
- Neff, P. and Bertler, N.: Trajectory modeling of modern dust transport to the Southern Ocean and 600 Antarctica, *J. Geophys. Res.-Atmos.*, 120, 9303-9322, 10.1002/2015JD023304, 2015.
- Nishizawa, T., Okamoto, H., Sugimoto, N., Matsui, I., Shimizu, A., and Aoki, K.: An algorithm that retrieves aerosol properties from dual-wavelength polarized lidar measurements, *Journal of Geophysical Research-Atmospheres*, 112, 10.1029/2006jd007435, 2007.
- Ogunjobi, K., He, Z., and Simmer, C.: Spectral aerosol optical properties from AERONET 605 Sun-photometric measurements over West Africa, *Atmospheric Research*, 88, 89-107, 10.1016/j.atmosres.2007.10.004, 2008.
- Omar, A., Won, J., Winker, D., Yoon, S., Dubovik, O., and McCormick, M.: Development of global aerosol models using cluster analysis of Aerosol Robotic Network (AERONET) measurements, *Journal of Geophysical Research-Atmospheres*, 110, 10.1029/2004jd004874, 2005.
- 610 Peyridieu, S., Chedin, A., Tanre, D., Capelle, V., Pierangelo, C., Lamquin, N., and Armante, R.: Saharan dust infrared optical depth and altitude retrieved from AIRS: a focus over North Atlantic - comparison to MODIS and CALIPSO, *Atmospheric Chemistry and Physics*, 10, 1953-1967, 10.5194/acp-10-1953-2010, 2010.
- Pokharel, M., Guang, J., Liu, B., Kang, S., Ma, Y., Holben, B., Xia, X., Xin, J., Ram, K., Rupakheti, D., 615 Wan, X., Wu, G., Bhattarai, H., Zhao, C., and Cong, Z.: Aerosol Properties Over Tibetan Plateau From



- a Decade of AERONET Measurements: Baseline, Types, and Influencing Factors, *Journal of Geophysical Research-Atmospheres*, 124, 13357-13374, 10.1029/2019jd031293, 2019.
- Rap, A., Scott, C., Spracklen, D., Bellouin, N., Forster, P., Carslaw, K., Schmidt, A., and Mann, G.: Natural aerosol direct and indirect radiative effects, *Geophysical Research Letters*, 40, 3297-3301, 620 10.1002/grl.50441, 2013.
- Qunn, P., Coffman, D., Kapustin, V., Bates, V., and Covert, D.: Aerosol optical properties in the marine boundary layer during the First Aerosol Characterization Experiment (ACE 1) and the underlying chemical and physical aerosol properties, *Journal of Geophysical Research-Atmospheres*, 103, 16547-16563, 10.1029/97JD02345, 1998.
- 625 Ravi, S., D'Odorico, P., Breshears, D., Field, J., Goudie, A., Huxman, T., Li, J., Okin, G., Swap, R., Thomas, A., Van Pelt, S., Whicker, J., and Zobeck, T.: Aeolian process and the biosphere, *Reviews of Geophysics*, 49, 10.1029/2010rg000328, 2011.
- Righi, M., Klinger, C., Eyring, V., Hendricks, J., Lauer, A., and Petzold, A.: Climate Impact of Biofuels in Shipping: Global Model Studies of the Aerosol Indirect Effect, *Environmental Science & 630 Technology*, 45, 3519-3525, 10.1021/es1036157, 2011.
- Rousseau, D., Schevin, P., Duzer, D., Cambon, G., Ferrier, J., Jolly, D., and Poulsen, U.: New evidence of long distance pollen transport to southern Greenland in late spring, *Review of Palaeobotany and Palynology*, 141, 277-286, 10.1016/j.revpalbo.2006.05.001, 2006.
- Russell, P., Kacenelenbogen, M., Livingston, J., Hasekamp, O., Burton, S., Schuster, G., Johnson, M., 635 Knobelspiesse, K., Redemann, J., Ramachandran, S., and Holben, B.: A multiparameter aerosol classification method and its application to retrievals from spaceborne polarimetry, *Journal of Geophysical Research-Atmospheres*, 119, 9838-9863, 10.1002/2013jd021411, 2014.
- Schmeisser, L., Backman, J., Ogren, J., Andrews, E., Asmi, E., Starkweather, S., Uttal, T., Fiebig, M., Sharma, S., Eleftheriadis, K., Vratolis, S., Bergin, M., Tunved, P., and Jefferson, A.: Seasonality of 640 aerosol optical properties in the Arctic, *Atmospheric Chemistry and Physics*, 18, 11599-11622, 10.5194/acp-18-11599-2018, 2018.
- Seinfeld, J., Bretherton, C., Carslaw, K., Coe, H., DeMott, P., Dunlea, E., Feingold, G., Ghan, S., Guenther, A., Kahn, R., Kraucunas, I., Kreidenweis, S., Molina, M. J., Nenes, A., Penner, J., Prather,



- 645 K., Ramanathan, V., Ramaswamy, V., Rasch, P., Ravishankara, A., Rosenfeld, D., Stephens, G., and  
Wood, R.: Improving our fundamental understanding of the role of aerosol-cloud interactions in the  
climate system, *Proceedings of the National Academy of Sciences of the United States of America*, 113,  
5781-5790, 10.1073/pnas.1514043113, 2016.
- Sharma, S., Ishizawa, M., Chan, D., Lavoue, D., Andrews, E., Eleftheriadis, K., and Maksyutov, S.:  
16-year simulation of Arctic black carbon: Transport, source contribution, and sensitivity analysis on  
650 deposition, *Journal of Geophysical Research-Atmospheres*, 118, 943-964, 10.1029/2012jd017774,  
2013.
- Shimizu, A., Nishizawa, T., Jin, Y., Kim, S.-W., Wang, Z., Batdorj, D., and Sugimoto, N.: Evolution of  
a lidar network for tropospheric aerosol detection in East Asia, *Optical Engineering*, 56,  
10.1117/1.Oe.56.3.031219, 2017.
- 655 Soja, A., Cofer, W., Shugart, H., Sukhinin, A., Stackhouse, P., McRae, D., and Conard, S.: Estimating  
fire emissions and disparities in boreal Siberia (1998-2002), *Journal of Geophysical  
Research-Atmospheres*, 109, 10.1029/2004jd004570, 2004.
- Stein, A., Draxler, R., Rolph, G., Stunder, B., Cohen, M., and Ngan, F.: NOAA'S HYSPLIT  
atmospheric transport and dispersion modeling system, *Bulletin of the American Meteorological  
660 Society*, 96, 2059-2077, 10.1175/bams-d-14-00110.1, 2015.
- Stohl, A., Andrews, E., Burkart, J., Forster, C., Herber, A., Hoch, S., Kowal, D., Lunder, C., Mefford,  
T., Ogren, J. A., Sharma, S., Spichtinger, N., Stebel, K., Stone, R., Strom, J., Torseth, K., Wehrli, C.,  
and Yttri, K. E.: Pan-Arctic enhancements of light absorbing aerosol concentrations due to North  
American boreal forest fires during summer 2004, *Journal of Geophysical Research-Atmospheres*, 111,  
665 10.1029/2006jd007216, 2006.
- Stone, R., Sharma, S., Herber, A., Eleftheriadis, K. and Nelson, D.: A characterization of Arctic  
aerosols on the basis of aerosol optical depth and black carbon measurements, *Elementa Science of the  
Anthropocene*, 2, p.000027, 10.12952/journal.elementa.000027, 2014.
- Sun, T., Che, H., Qi, B., Wang, Y., Dong, Y., Xia, X., Wang, H., Gui, K., Zheng, Y., Zhao, H., Ma, Q.,  
670 Du, R., and Zhang, X.: Aerosol optical characteristics and their vertical distributions under enhanced





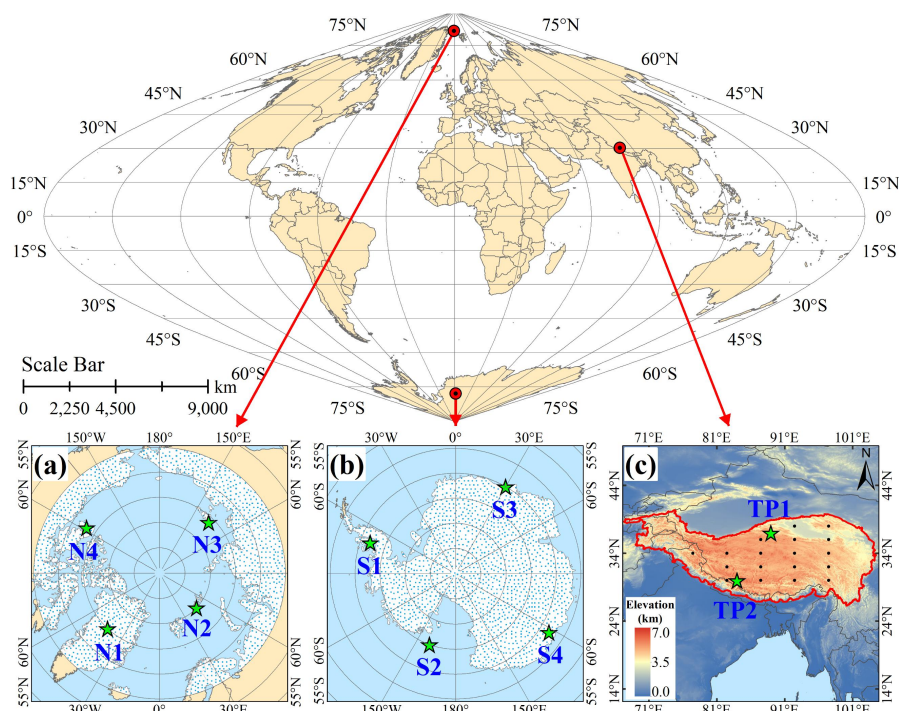
- haze pollution events: effect of the regional transport of different aerosol types over eastern China, *Atmospheric Chemistry and Physics*, 18, 2949-2971, 10.5194/acp-18-2949-2018, 2018.
- Tackett, J., Winker, D., Getzewich, B., Vaughan, M., Young, S., and Kar, J.: CALIPSO lidar level 3 aerosol profile product: version 3 algorithm design, *Atmospheric Measurement Techniques*, 11, 4129-4152, 10.5194/amt-11-4129-2018, 2018.
- Teinilä, K., Frey, A., Hillamo, R., Tuelp, H. C., and Weller, R.: A study of the sea-salt chemistry using size-segregated aerosol measurements at coastal Antarctic station Neumayer, *Atmospheric Environment*, 96, 11-19, 10.1016/j.atmosenv.2014.07.025, 2014.
- Tomasi, C., Vitale, V., Lupi, A., Di Carmine, C., Campanelli, M., Herber, A., Treffeisen, R., Stone, R., Andrews, E., Sharma, S., Radionov, V., von Hoyningen-Huene, W., Stebel, K., Hansen, G., Myhre, C., Wehrli, C., Aaltonen, V., Lihavainen, H., Virkkula, A., Hillamo, R., Stroem, J., Toledano, C., Cachorro, V., Ortiz, P., de Frutos, A., Blindheim, S., Frioud, M., Gausa, M., Zielinski, T., Petelski, T., and Yamanouchi, T.: Aerosols in polar regions: A historical overview based on optical depth and in situ observations, *Journal of Geophysical Research-Atmospheres*, 112, 10.1029/2007jd008432, 2007.
- Twomey, S.: Influence of pollution on shortwave albedo of clouds, *Journal of the Atmospheric Sciences*, 34, 1149-1152, 10.1175/1520-0469(1977)034<1149:Tiopot>2.0.Co;2, 1977.
- VanCuren, R., Cahill, T., Burkhart, J., Barnes, D., Zhao, Y., Perry, K., Cliff, S., and McConnell, J.: Aerosols and their sources at Summit Greenland - First results of continuous size- and time-resolved sampling, *Atmospheric Environment*, 52, 82-97, 10.1016/j.atmosenv.2011.10.047, 2012.
- Varnai, T., and Marshak, A.: Global CALIPSO Observations of Aerosol Changes Near Clouds, *Ieee Geoscience and Remote Sensing Letters*, 8, 19-23, 10.1109/lgrs.2010.2049982, 2011.
- Vernon, C., Bolt, R., Canty, T., and Kahn, R.: The impact of MISR-derived injection height initialization on wildfire and volcanic plume dispersion in the HYSPLIT model, *Atmospheric Measurement Techniques*, 11, 6289-6307, 10.5194/amt-11-6289-2018, 2018.
- Virkkula, A., Teinila, K., Hillamo, R., Kerminen, V. M., Saarikoski, S., Aurela, M., Viidanoja, J., Paatero, J., Koponen, I. K., and Kulmala, M.: Chemical composition of boundary layer aerosol over the Atlantic Ocean and at an Antarctic site, *Atmospheric Chemistry and Physics*, 6, 3407-3421, 10.5194/acp-6-3407-2006, 2006.



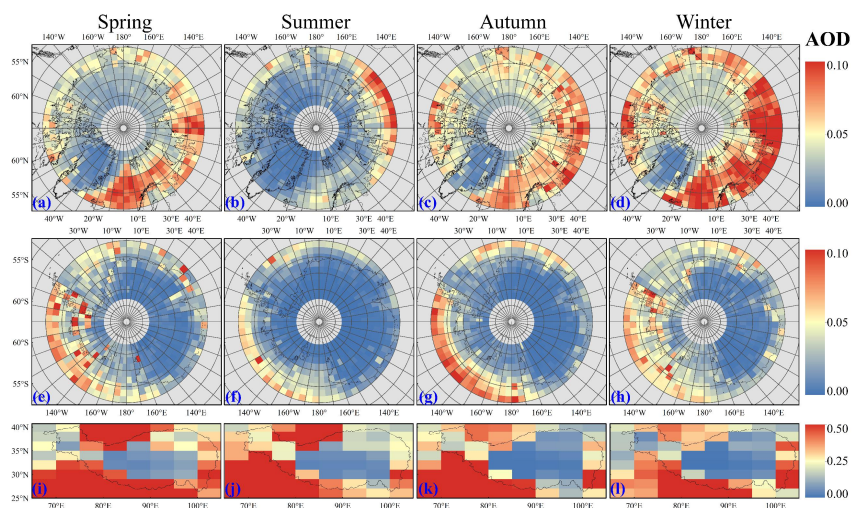
- 700 Wagenbach, D., Ducroz, F., Mulvaney, R., Keck, L., Minikin, A., Legrand, M., Hall, J., and Wolff, E.:  
Sea-salt aerosol in coastal Antarctic regions, *Journal of Geophysical Research-Atmospheres*, 103,  
10961-10974, 10.1029/97jd01804, 1998.
- Wang, Y., Jiang, J., Su, H., Choi, Y., Huang, L., Guo, J., and Yung, Y.: Elucidating the Role of  
Anthropogenic Aerosols in Arctic Sea Ice Variations, *Journal of Climate*, 31, 99-114,  
10.1175/jcli-d-17-0287.1, 2018.
- 705 Warneke, C., Froyd, K., Brioude, J., Bahreini, R., Brock, C., Cozic, J., de Gouw, J., Fahey, D., Ferrare,  
R., Holloway, J., Middlebrook, A., Miller, L., Montzka, S., Schwarz, J., Sodemann, H., Spackman, J.,  
and Stohl, A.: An important contribution to springtime Arctic aerosol from biomass burning in Russia,  
*Geophys. Res. Lett.*, 37, L01801, 10.1029/2009gl041816, 2010.
- Weller, R., Minikin, A., Petzold, A., Wagenbach, D., and König-Langlo, G.: Characterization of  
710 long-term and seasonal variations of black carbon (BC) concentrations at Neumayer, Antarctica,  
*Atmospheric Chemistry and Physics*, 13, 1579-1590, 10.5194/acp-13-1579-2013, 2013.
- Winker, D., Hunt, W., and McGill, M.: Initial performance assessment of CALIOP, *Geophysical  
Research Letters*, 34, 10.1029/2007gl030135, 2007.
- Winker, D., Pelon, J., Coakley Jr, J., Ackerman, S., Charlson, R., Colarco, P., Flamant, P., Fu, Q., Hoff,  
715 R., Kittaka, C., Kubar, T., Le Treut, H., McCormick, M., Megie, G., Poole, L., Powell, K., Trepte, C.,  
Vaughan, M., and Wielicki, B.: The CALIPSO mission a global 3D View of Aerosols and Clouds,  
*Bulletin of the American Meteorological Society*, 91, 1211-1229, 10.1175/2010bams3009.1, 2010.
- Winker, D., Tackett, J., Getzewich, B., Liu, Z., Vaughan, M., and Rogers, R.: The global 3-D  
distribution of tropospheric aerosols as characterized by CALIOP, *Atmos. Chem. Phys.*, 13, 3345-3361,  
720 <https://doi.org/10.5194/acp-13-3345-2013>, 2013.
- Wu, G., Wan, X., Gao, S., Fu, P., Yin, Y., Li, G., Zhang, G., Kang, S., Ram, K., and Cong, Z.:  
Humic-Like Substances (HULIS) in Aerosols of Central Tibetan Plateau (Nam Co, 4730 m asl):  
Abundance, Light Absorption Properties, and Sources, *Environmental Science & Technology*, 52,  
7203-7211, 10.1021/acs.est.8b01251, 2018.



- 725 Xia, X., Zong, X., Cong, Z., Chen, H., Kang, S., and Wang, P.: Baseline continental aerosol over the central Tibetan plateau and a case study of aerosol transport from South Asia, *Atmospheric Environment*, 45, 7370-7378, 10.1016/j.atmosenv.2011.07.067, 2011.
- Xing, J., Wang, J., Mathur, R., Wang, S., Sarwar, G., Pleim, J., Hogrefe, C., Zhang, Y., Jiang, J., Wong, D. C., and Hao, J.: Impacts of aerosol direct effects on tropospheric ozone through changes in atmospheric dynamics and photolysis rates, *Atmospheric Chemistry and Physics*, 17, 9869-9883, 10.5194/acp-17-9869-2017, 2017.
- Xu, C., Ma, Y., Panday, A., Cong, Z., Yang, K., Zhu, Z., Wang, J., Amatya, P., and Zhao, L.: Similarities and differences of aerosol optical properties between southern and northern sides of the Himalayas, *Atmospheric Chemistry and Physics*, 14, 3133-3149, 10.5194/acp-14-3133-2014, 2014.
- 735 Xu, C., Ma, Y., You, C., and Zhu, Z.: The regional distribution characteristics of aerosol optical depth over the Tibetan Plateau, *Atmospheric Chemistry and Physics*, 15, 12065-12078, 10.5194/acp-15-12065-2015, 2015.
- Zhao, C., and Garrett, T.: Effects of Arctic haze on surface cloud radiative forcing, *Geophysical Research Letters*, 42, 557-564, 10.1002/2014gl062015, 2015.
- 740 Zhao, C., Andrews, A., Bianco, L., Eluszkiewicz, J., Hirsch, A., MacDonald, C., Nehrkom, T., and Fischer, M.: Atmospheric inverse estimates of methane emissions from Central California, *Journal of Geophysical Research-Atmospheres*, 114, 10.1029/2008jd011671, 2009.
- Zhao, C., Yang, Y., Fan, H., Huang, J., Fu, Y., Zhang, X., Kang, S., Cong, Z., Letu, H., and Menenti, M.: Aerosol characteristics and impacts on weather and climate over the Tibetan Plateau, *National Science Review*, 7, 492-+, 10.1093/nsr/nwz184, 2020.
- 745 Zou, X., Hou, S., Liu, K., Yu, J., Zhang, W., Pang, H., Hua, R., and Mayewski, P.: Uranium record from a 3 m snow pit at Dome Argus, East Antarctica, *Plos One*, 13, 10.1371/journal.pone.0206598, 2018.



750 **Figure 1:** Geographical map of the three study areas, (a) Arctic, (b) Antarctic, and (c) TP. Among them, the  
white background and blue pints represent the land within the study area. In (c), the black dots represent  
the center of the TP inner pixel corresponding to CALIPSO L3 aerosol data, the green pentagrams  
represent the site of aerosol back trajectory study, the red line represents the boundary of the TP, and the  
color represents the surface elevation data from Shuttle Radar Topography Mission (SRTM) on  
755 <http://srtm.csi.cgiar.org/>.



760 **Figure 2: Seasonal averaged AOD distribution for thirteen years (2006 ~ 2019) over the Arctic, Antarctic, and TP. Four columns represent four seasons. (a) ~ (d), (e) ~ (h), and (i) ~ (l) represent the spatial distribution of aerosols in the Arctic, Antarctic, and TP, respectively.**

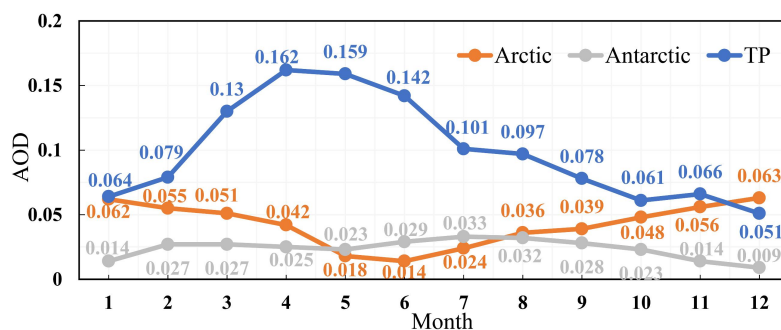
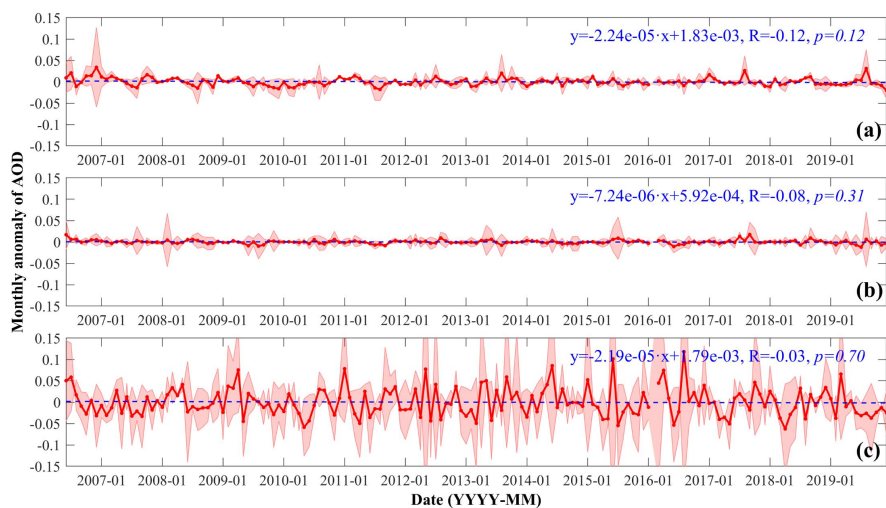
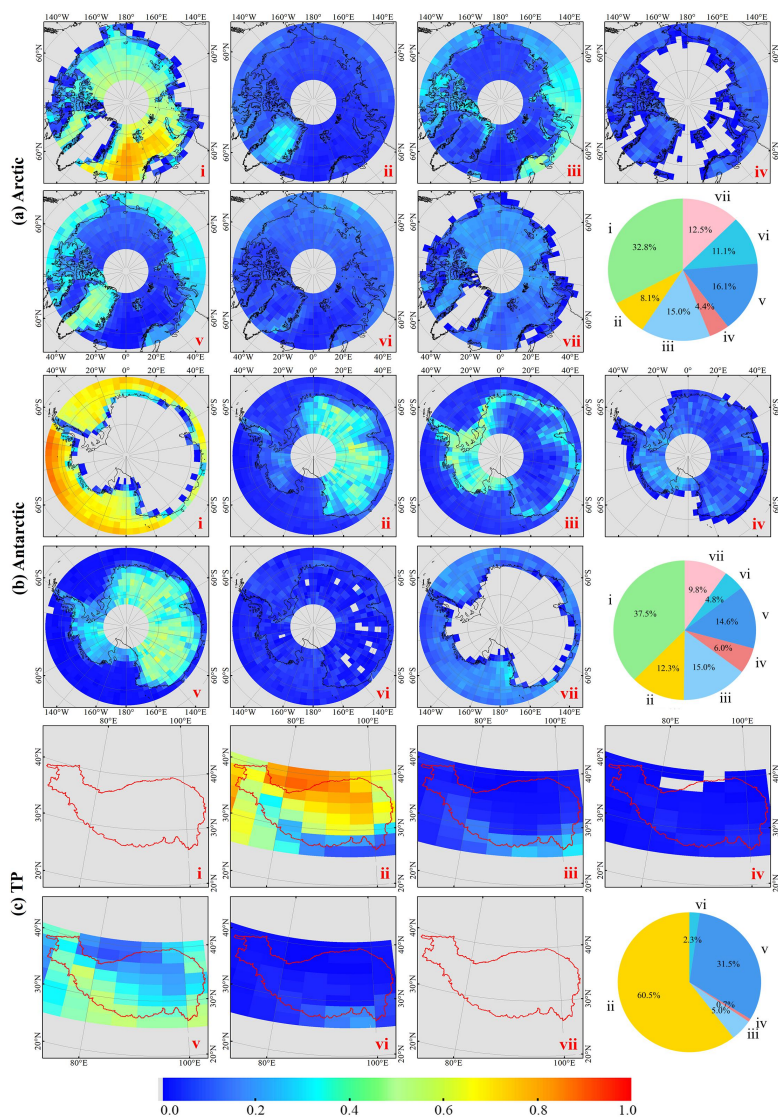


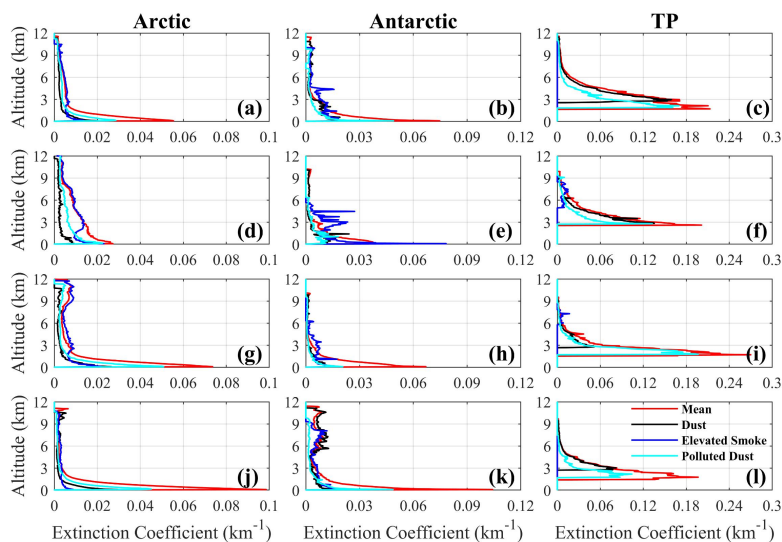
**Figure 3: Monthly averaged AOD over the Arctic, Antarctic, and TP.**



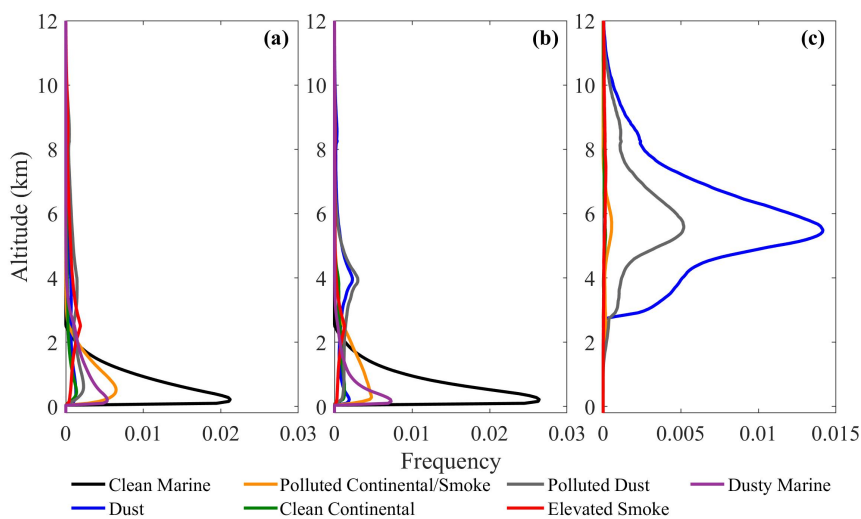
765 **Figure 4: Temporal variation of monthly AOD anomalies from June 2006 to December 2019 over the (a) Arctic, (b) Antarctic, and (c) TP. The red solid lines and shadows represent the deseasonalized monthly AOD anomalies and standard deviations, respectively, while the blue dotted lines represent the linear trends.**



770 **Figure 5:** The annual averaged OF maps for seven aerosol types defined by CALIOP products over the (a) Arctic, (b) Antarctic, and (c) TP. The number i ~ vii represent clean marine, dust, polluted continental/smoke, clean continental, polluted dust, elevated smoke, and dusty marine, respectively. The pie represents the annual average OF of all pixels for seven aerosol types.



775 **Figure 6:** The vertical distribution of the seasonal (Spring: (a) ~ (c); Summer: (d) ~ (f); Autumn: (g) ~ (i); Winter: (j) ~ (l)) averaged aerosol extinction coefficient at 532 nm over the Arctic (left panel), Antarctic (middle panel), and TP (right panel), including the mean extinction coefficient (red solid line), dust extinction coefficient (black solid line), Elevated smoke extinction coefficient (blue solid line), and polluted dust extinction coefficient (cyan solid line) over the Arctic (a, d, g, and j), Antarctic (b, e, h, and k), and TP (c, f, i, and l).



780 **Figure 7:** The vertical distribution of OF of aerosol types over the (a) Arctic, (b) Antarctic, and (c) TP.



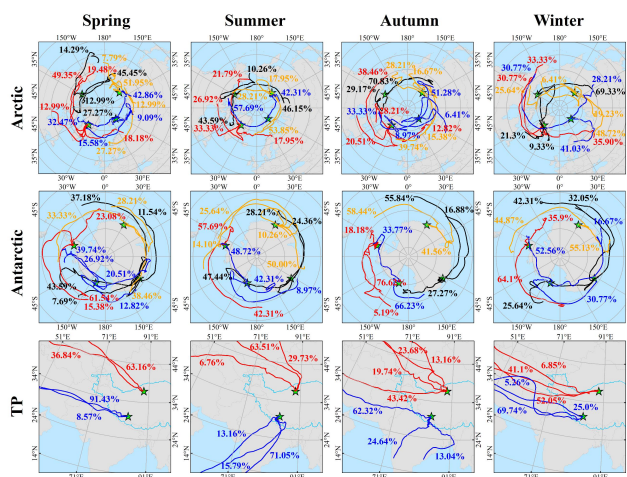


Figure 8: The back trajectories at each of the Arctic, Antarctic, and TP sites, separated by spring, summer, autumn, and winter.

785



**Table 1: The normalized seasonal averaged OF of seven aerosol types over the Arctic, Antarctic, and TP.**

Region	Season	Aerosol Types						
		Clean marine	Dust	Polluted continental /smoke	Clean continental	Polluted dust	Elevated smoke	Dusty marine
Arctic	Spring	0.244	0.113	0.119	0.045	0.231	0.125	0.123
	Summer	0.131	0.041	0.192	0.051	0.184	0.342	0.059
	Autumn	0.418	0.067	0.143	0.049	0.124	0.107	0.092
	Winter	0.371	0.073	0.163	0.041	0.134	0.069	0.149
Antarctic	Spring	0.344	0.143	0.154	0.054	0.137	0.052	0.116
	Summer	0.612	0.137	0.082	0.007	0.052	0.021	0.089
	Autumn	0.34	0.139	0.144	0.069	0.200	0.043	0.065
	Winter	0.359	0.096	0.169	0.070	0.133	0.056	0.117
TP	Spring	0.000	0.731	0.015	0.004	0.238	0.012	0.000
	Summer	0.000	0.714	0.021	0.005	0.244	0.016	0.000
	Autumn	0.000	0.554	0.053	0.008	0.361	0.024	0.000
	Winter	0.000	0.331	0.144	0.014	0.463	0.048	0.000